*Reprinted from:*

# computer programs in biomedicine

an international journal devoted to the exchange of information on computer programs used in biomedical research

Volume 1, No. 2, June 1970

## COMPUTER SIMULATION OF FERROKINETIC MODELS*

Torgny GROTH and Werner SCHNEIDER
*Uppsala Data Center, University of Uppsala, Sweden*

Erik SANDEWALL
*Department of Computer Sciences, University of Uppsala, Sweden*

and

Jean-Claude VUILLE
*Department of Pediatrics, University Hospital, University of Uppsala, Sweden*

pp. 90–104

NORTH-HOLLAND PUBLISHING COMPANY – AMSTERDAM

COMPUTER PROGRAMS IN BIOMEDICINE 1 (1970) 90–104. NORTH-HOLLAND PUBLISHING COMPANY

# COMPUTER SIMULATION OF FERROKINETIC MODELS*

Torgny GROTH and Werner SCHNEIDER
*Uppsala Data Center, University of Uppsala, Sweden*

Erik SANDEWALL
*Department of Computer Sciences, University of Uppsala, Sweden*

and

Jean-Claude VUILLE
*Department of Pediatrics, University Hospital, University of Uppsala, Sweden*

Computer methods for analysis of iron kinetics on the basis of specified models are presented. One method is based on direct simulation of the processes in the model, whereas the other method uses a standard fourth-order Runge – Kutta integration of the system of differential equations describing the model.

Simulation Ferrokinetic Models

## 1. Introduction and computational methods

Observation of the behaviour in plasma and red cells of intravenously injected radioiron form a basis for the study of iron-kinetics in man. The theoretical interpretation of the experimental data can be derived from different ferrokinetic models consisting of various iron pools and flows connected to the plasma compartment in various manners. In the original paper by Garby et al. [1] a relatively simple model was presented which could be formulated mathematically in terms of analytically solvable differential equations. This model was in many respects similar to that proposed in 1961 by Pollycove and Mortimer [2]. Further investigations [3,4], however, especially on the bone marrow part of the model, demonstrated the necessity of analysing models of different basic structure. The introduction of more sophisticated mechanisms, simulating maturation *of* and iron uptake *by* red cell precursors in the bone marrow, as well as premature death of newly formed red cells, necessitated the use of new computer techniques, since it was no longer possible to solve the differential equations analytically. The purpose of this paper is to illustrate two suitable computer methods for the simulation of this kind of process, to be used in the cyclic search for adequate models, including experiments, data reduction, formulation of models, parameter estimation and simulation of new experiments.

In the first method (A) the simulation is performed in small time intervals $\Delta t$ and the change $\Delta x$ in each compartment $x$ is calculated from the system of differential equations describing the system by approximating the derivatives by quotients of differences $\Delta x/\Delta t$. The other method (B) is based on the solution of the system of differential equations by a standard fourth order Runge – Kutta algorithm. For a detailde review of different methods for the simulation of continuous systems see ref. [5].

Method A has two interdependent drawbacks for routine use. In order to obtain high accuracy, the time intervals used in the simulation procedure must be very small, a requirement which increases the computer time needed for the production of one set of

* This work was supported in part by the Swedish Natural Science Research Council.

theoretical curves. Using method B larger time intervals can be chosen for the same level of accuracy, thereby reducing the total number of steps at which calculations have to be performed.

Both methods are able to yield valid theoretical curves for a specified model, but it may be recommended to use the simple procedure of method A when several models are to be studied, e.g. with respect to their compatibility with experimental data. Once a specified model is accepted for further work, which often implies the production of a large number of theoretical curves (parameter estimation by curve fitting), a more powerful procedure like method B should be applied. From the point of view of the ease and the flexibility of the programming technique, however, method A is clearly superior to method B. Available general programs for the analysis of multi-compartment systems, e.g. [6,7] (for an excellent review see [5]), have not been used, in order to preserve full flexibility in the simulation of the sophisticated mechanisms of maturation in the bone marrow and premature death of newly formed red cells. Automatic choice of step length in the integration to obtain a desired accuracy has not been implemented in the programs because of the relative ease to make this choice manually in this kind of problem.

In order to compare the results obtained by the methods of numerical integration with analytical solutions, the simple but "incompatible" model of Garby et al. [1] has been used. In the present paper this model will be called *model 1* (see fig. 1). The "compatible" model IIc according to Vuille [3] will be called *model 2* (see fig. 2). The interpretation of the symbols is given below. It is to be noticed that the exchange between the red cell compartment C and the S-compartment is very slow (the normal life span of red cells is c. 120 days) and has not been considered in the model that concerns the evaluation of rate constants. For further details, the reader is referred to the previous papers [1,3,4]. The process of premature death of newly formed red cells deserves some further comment. This process occurs both in normal individuals and haematological disorders [8-10], but the detailed mechanisms leading to early destruction of cells are not well known. It seems reasonable to assume that the red cell precursors destined for premature death represent a population that differs in certain respects from "normal" cells already at the earliest stages of maturation. If this assumption is correct, this population of precursors should be separated in the model from the population of cells that survive normally. Such a model, including two different populations of red cell precursors, will be treated as well in the present paper (*model 3*, fig. 3).

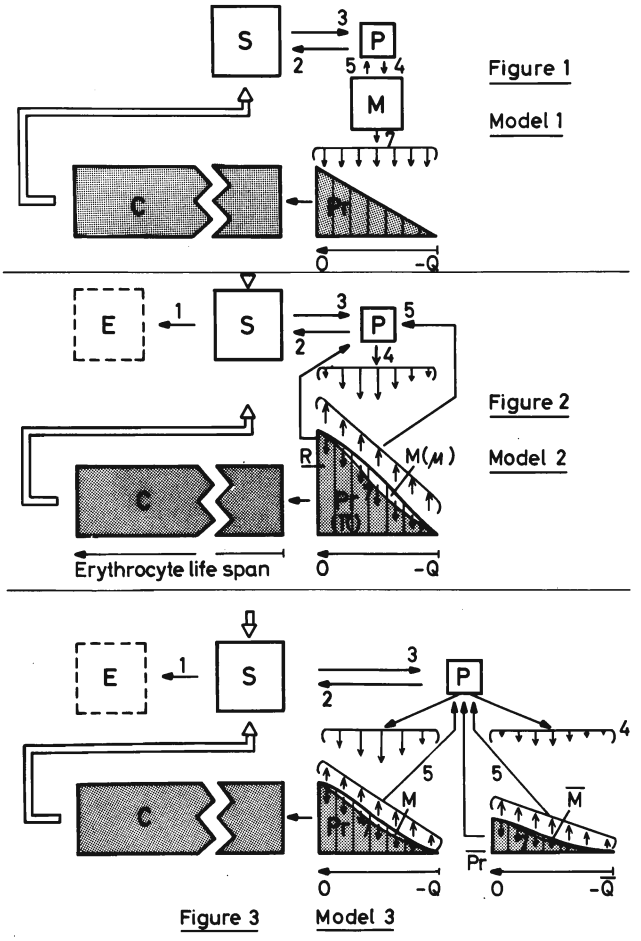


Figs. 1–3. Models 1–3. For explanation of symbols see text.

The following variables will be used:

- $t$ : Time after injection of the tracer.
- $v$ : Time variable, indicating the time of delivery to the circulation of a certain set of precursors.
- $E(t)$ : Amount of radioiron excreted from the body and/or fixed irreversibly in storage.
- $S(t)$ : Amount of radioiron stored reversibly in liver, spleen etc.
- $P(t)$ : Amount of radioiron in plasma.
- $C(t)$ : Amount of radioiron in circulating red cells.

$\pi(t,\upsilon)$ : Amount of haem-radioiron (at time $t$) in the precursors that will be delivered to the circulation ($C$) at time $\upsilon$.

$\mu(t,\upsilon)$ : Amount of exchangeable non-haem-radioiron (at time $t$) in the precursors that will be delivered to the circulation ($C$) at time $\upsilon$.

$\bar{\pi}(t,\upsilon)$ : Corresponding quantities for precursors

$\bar{\mu}(t,\upsilon)$ that will die prematurely and deliver their iron content directly to the plasma. (In the following called "sick" precursors in contrast to "normal" precursors.)

$Q$ : Maturation time for normal precursors.

$\bar{Q}$ : Maturation time for "sick" precursors.

$\omega(t-\upsilon)$ : Distribution function for the iron flow from $P$ to $\mu$. Note that $t-\upsilon$ is the age of the corpuscle, being $-Q$ when the precursor is "created" and 0 when the precursor enters the blood stream. It follows that $\omega \neq 0$ for arguments between $-Q$ and 0.

$\bar{\omega}(t-\upsilon)$ : Corresponding distribution function for flow from $P$ to $\bar{\mu}$. $\bar{\omega} \neq 0$ for arguments between $-Q$ and 0.

$R = \int_{-\bar{Q}}^{0} \bar{\omega}(t)\mathrm{d}t$ : denotes the fraction of the iron flowing from $P$ to the sick precursors. Moreover, it follows that $\int_{-\bar{Q}}^{0} \omega(t)\mathrm{d}t = 1 - R$.

$K_i$ : Rate constants. Subscripts according to the numbers of the arrows in fig. 2 and fig. 3. $K_5$ and $K_7$ are in the present context assumed to be identical for "normal" and "sick" precursors, though this is not a requirement for the theoretical analysis.

In the simplified model 2, no distinction is made between $\mu$ and $\bar{\mu}$, or between $\pi$ and $\bar{\pi}$. Instead, a fraction $R$ of the precursors ready to leave the bone marrow are destroyed, and their iron is returned to $P$. In this case, we obtain the following system of differential equations:

$$\frac{\mathrm{d}E}{\mathrm{d}t} = K_1 S \,. \tag{2.1}$$

$$\frac{\mathrm{d}S}{\mathrm{d}t} = K_2 P - (K_1 + K_3) S \,. \tag{2.2}$$

$$\frac{\mathrm{d}\pi}{\mathrm{d}t} = K_7 \mu \,. \tag{2.3}$$

$$\frac{\mathrm{d}\mu}{\mathrm{d}t} = K_4 P\, \omega(t-\upsilon) - (K_5 + K_7)\mu \,. \tag{2.5}$$

$$\frac{\mathrm{d}C}{\mathrm{d}t} = (1-R)\,[\mu(t,t) + \pi(t,t)] \,. \tag{2.7}$$

$$\frac{\mathrm{d}P}{\mathrm{d}t} = K_3 S - (K_2 + K_4) P + R\,[\mu(t,t) + \pi(t,t)] + K_5 \int_t^{t+Q} \mu(t,\upsilon)\,\mathrm{d}\upsilon \,. \tag{2.8}$$

Model 3 yields the following differential equations:

$$\frac{\mathrm{d}E}{\mathrm{d}t} = K_1 S \,. \tag{3.1}$$

$$\frac{\mathrm{d}S}{\mathrm{d}t} = K_2 P - (K_1 + K_3) S \,. \tag{3.2}$$

$$\frac{\mathrm{d}\pi}{\mathrm{d}t} = K_7 \mu \,; \tag{3.3}$$

$$\frac{\mathrm{d}\bar{\pi}}{\mathrm{d}t} = K_7 \bar{\mu} \,. \tag{3.4}$$

$$\frac{\mathrm{d}\mu}{\mathrm{d}t} = K_4 P\, \omega(t-\upsilon) - (K_5 + K_7)\mu \,. \tag{3.5}$$

$$\frac{\mathrm{d}\bar{\mu}}{\mathrm{d}t} = K_4 P\, \bar{\omega}(t-\upsilon) - (K_5 + K_7)\bar{\mu} \,. \tag{3.6}$$

$$\frac{\mathrm{d}C}{\mathrm{d}t} = \mu(t,t) + \pi(t,t) \,. \tag{3.7}$$

$$\frac{\mathrm{d}P}{\mathrm{d}t} = K_3 S - (K_2 + K_4) P + \bar{\mu}(t,t) + \bar{\pi}(t,t) + K_5 \left[\int_t^{t+Q} \mu(t,\upsilon)\,\mathrm{d}\upsilon + \int_t^{t+\bar{Q}} \bar{\mu}(t,\upsilon)\,\mathrm{d}\upsilon\right] . \tag{3.8}$$

It should be noted that if $\omega(t-\upsilon) = a\bar{\omega}(t-\upsilon)$, where $a$ is a constant, the systems (2) and (3) are equivalent. In this case, we must have $Q = \bar{Q}$. The systems of differential equations (2.1)–(2.8) and (3.1)–(3.8) cannot be solved to yield analytical expressions for the amount of radioiron contained in each compartment at any time $t$ (as was the case for model 1, cf. [1]). The systems may be solved, however, by conventional methods of numerical integration [5], e.g. Runge – Kutta algorithms of different orders. Suppose that for a given $t_n$ we know the values of $E$, $S$, $C$ and $P$, and that the values of $\mu$ and $\pi$ for this $t$ and all $\upsilon = pk$ ($p$ is an integer) are known. Moreover, suppose $\omega$ can be evaluated for any argument (according to an arbitrary function specified as input data). Checking through the systems of equations, we easily verify that the derivatives with respect to $t$ of all involved quantities can be computed.

Using method B, the handling of the parameter $\upsilon$ is

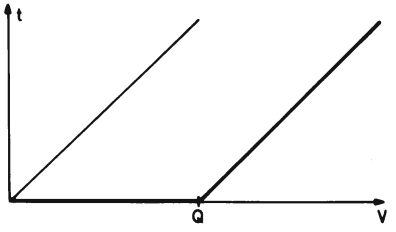


Fig. 4. The functions $\mu$, $\pi$, $\bar{\mu}$ and $\bar{\pi}$ are defined to satisfy the conditions $\mu(0,v) = \pi(0,v) = \bar{\mu}(0,v) = \bar{\pi}(0,v) = 0$ and $\mu(t,t+Q) = \pi(t,t+Q) = \bar{\mu}(t,t+\bar{Q}) = \bar{\pi}(t,t+\bar{Q}) = 0$ (fat lines).

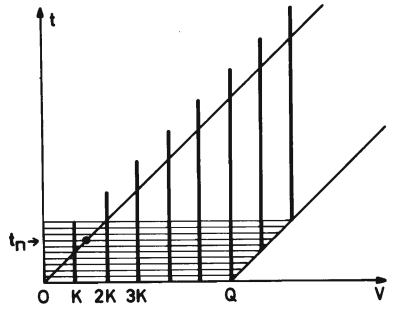


Fig. 5. To get an optimal compromise between accuracy and computer time, the intervals $k$ are made greater than the intervals $h$ in the $t$-direction. The dot represents the point $(nh,nh)$, which is found by interpolation.

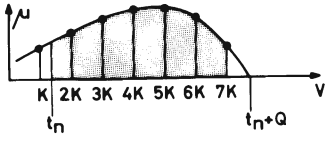


Fig. 6. The shadowed area represents the integral

$$\int_t^{t+Q} \mu(t,v)\,dv\,.$$

The heavy dots indicate known values of $\mu$.

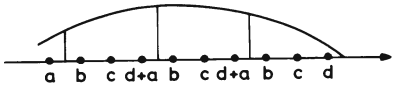


Fig. 7. The weights used in the fourth-order quadrature formula for $k = Q/9$.

not quite trivial. The functions $\mu$ and $\pi$ are defined on the strip $0 \leqslant v - t \leqslant Q$ (see fig. 4). Restricting the discussion to $\mu$, we have $\mu(0,v) = 0$ and $\mu(t,t+Q) = 0$ (fat lines in fig. 4). The case $\mu(0,v)$ describes the initial situation; the case $\mu(t,t+Q)$ the initiation of new precursors. A horizontal cross section in the figure describes the state of the $\mu$ pool at a fixed time $t$, for varying time of delivery $v$. A vertical cross section, on the other hand, describes the development through $t$ of precursors with a certain time of delivery $v$. Referring to the system (2), we see that eq. (2.5) describes the development of $\mu$ along such a vertical cross section. Eqs. (2.7) and (2.8) utilize the value of $\mu$ on the line $t = v$. Eq. (2.8) also uses the integral of $\mu$ over a horizontal cross section. In the procedure of numerical integration, $\mu$ has to be handled in discrete points. In order to obtain an optimal compromise between accuracy and computer time it is desirable that the intervals $k$ in the $v$ direction are greater than the intervals $h$ in the $t$ direction. This condition is shown schematically in fig. 5. At a fixed point $t_n = nh$ we may know the value of $\mu$ in points $(k,nh)$, $(2k,nh)$, $(3k,nh)$, ..., but due to the difference in interval length, we do not know explicitly the values of $\mu$ in the point $(nh,nh)$ which is used in eqs. (2.7) and (2.8). Of course, we can obtain the value of $\mu(nh,nh)$ by interpolation in the $v$ direction. In order to make this interpolation efficient, we have to integrate $\mu$ by (2.5) *beyond* the line $t = v$. The vertical lines in figure $k$ indicate how far we integrate. It should be noted that the value of $\mu(t,v)$ for $t > v$ has no physical significance, but that it is perfectly possible to use it in the computations. In equation (2.8) we need

$$\int_t^{t+Q} \mu(t,v)\,dv\,.$$

Considering a horizontal cross-section for $t = t_n$ in fig. 5 we obtain the desired integral as the shadowed area in fig. 6, where heavy dots indicate known values of $\mu$. A special fourth-order quadrature formula has been designed for the calculation of the desired integral. Let $\Delta$ be a measure of the skewness, defined by $t = (p+\Delta)k$, where $p$ is an integer and $0 \leqslant \Delta < 1$. For example, $\Delta = 0.5$ for $t_n = 3/2k$.

Next, define

$$\alpha = 3+6\Delta^2,\ \beta = 8\Delta+4\Delta^3,\ \gamma = 9-6\Delta^2,\ \delta = 12\Delta^3, \tag{3.9}$$

and

$$a = \tfrac{1}{8}(\alpha - \beta)\,,\quad b = \tfrac{1}{8}(\gamma + \delta)\,,$$
$$c = \tfrac{1}{8}(\gamma - \delta)\,,\quad d = \tfrac{1}{8}(\alpha + \beta)\,, \qquad (3.10)$$

it is easily verified that the formula

$$\int_{v+\Delta h}^{v+3h+\Delta h} f(t)\,dt \approx af(v) + bf(v+h) + cf(v+2h) + df(v+3h) \qquad (3.11)$$

gives the exact result if $f$ is a polynomial of order $\leqslant 3$. By iterated use of this formula we can obtain good approximation of

$$\int_{t}^{t+Q} \mu(t,v)\,dv$$

if $Q/k$ (the number of steps in the $v$ direction) is a multiple of 3. For instance, if $k = Q/9$ we must use the weights indicated in fig. 7. (Note that $d + a = \frac{1}{4}\alpha$. The function $\pi$ and the corresponding functions $\bar{\mu}$ and $\bar{\pi}$ are handled in the same way as $\mu$. As a check of the integration, the total sum of all the compartments is used in every timestep (conservation of amount of injected radioiron). Deviations greater than a specified size are printed out as error messages.

## 2. Basic flowcharts

The basic flowchart for method A is shown in fig.8. This flowchart applies to all three models in general. The bone marrow processers are, however, illustrated for model 1 and the last box in fig. 8 has to be modified in order to cover the details of models 2 and 3 (see figs. 1,2 and 3). As a detailed complement and in order to illustrate the simplicity of method A the corresponding FORTRAN program for model 3 is listed at the end of this paper. In fig. 9 a brief flowchart is given for method B as applied to model 3.

## 3. Typical sample runs

Sample runs will be given at the end of this paper for methods A and B. Model 3 has been chosen. Table 1 gives the parameters used in the computations.

Table 1
Parameters used in the computations

| Parameters | Model 1 | Model 3 |
|---|---|---|
| $k_1$ | 0.0000 | 0.05 |
| $k_2$ | 0.5482 | 1.50 |
| $k_3$ | 0.0555 | 0.15 |
| $k_4$ | 9.2478 | 7.50 |
| $k_5$ | 0.2064 | 2.00 |
| $k_7$ | 0.2920 | 9.00 |
| $R$ | | 0.100 |
| $Q$ | 6 | 7.50 |
| $\bar{Q}$ | - | - |
| $\omega$ | Rectangular distribution function | Triangular distribution function |

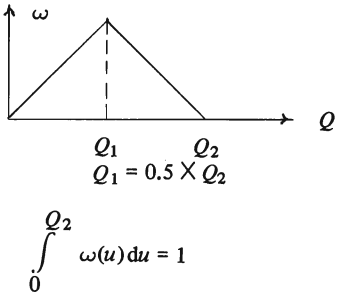


$$\int_0^{Q_2} \omega(u)\,du = 1$$

The theoretical radioiron curves in compartments $P$ (disappearance curve) and $C$ (appearance curve) are shown in figs. 10 and 11. As a visual illustration of the rate of convergence the disappearance curve is given as calculated with methods A and B using various step lengths. From these figures it can be seen that:

1. Both methods converge towards the same limit curve.

2. The Runge – Kutta method converges, as expected, more rapidly than the simulation method. In fact, the differences between the curves obtained with the Runge – Kutta method and step lengths from 0.001 to 0.05 day were so small that they could not be drawn in the figure.

3. The deviation between the two methods and between two curves with different steplengths is largest within the interval 0 – 1 day, while the differences are negligible after $t = 2$ days. The problem of accuracy in the integration can of course be managed by automatic step length control, but in order to reduce computer time needed in the calculation of a large num-

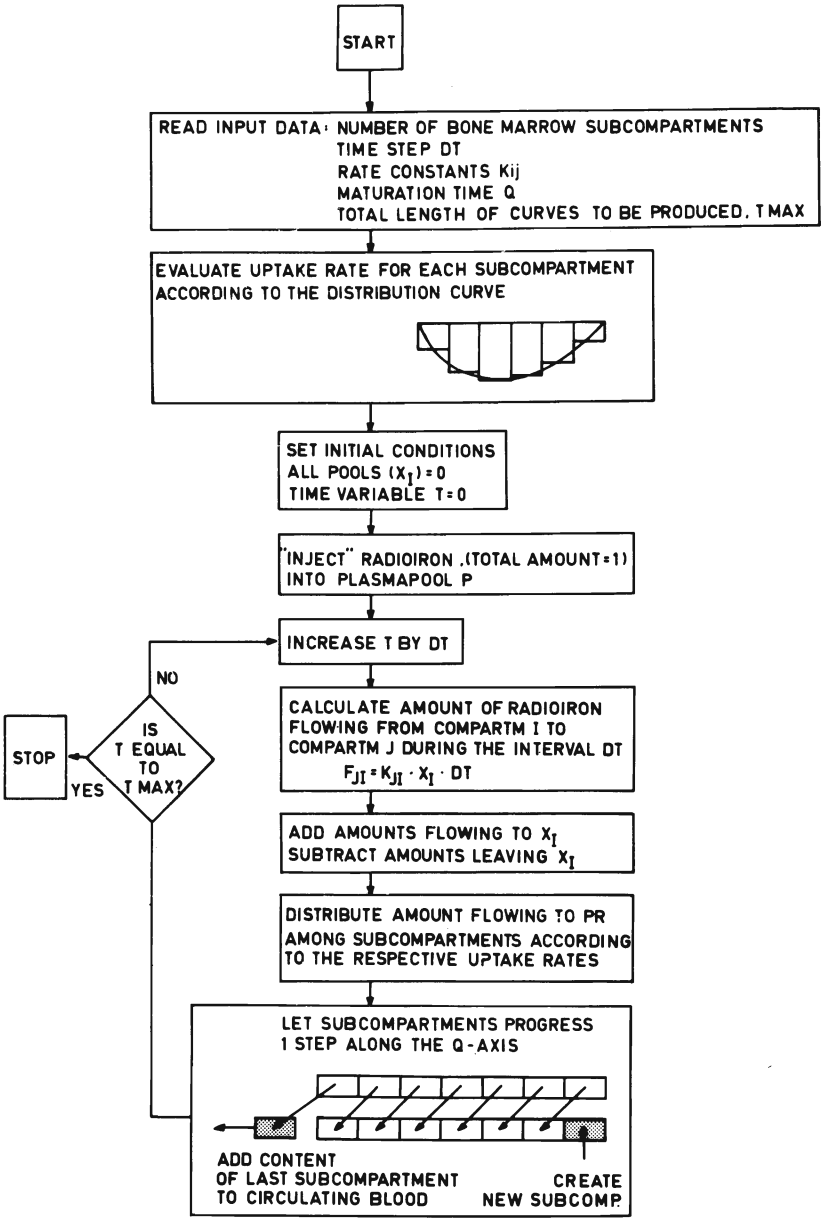


Fig. 8. The general principles of method A presented as a block-diagram.

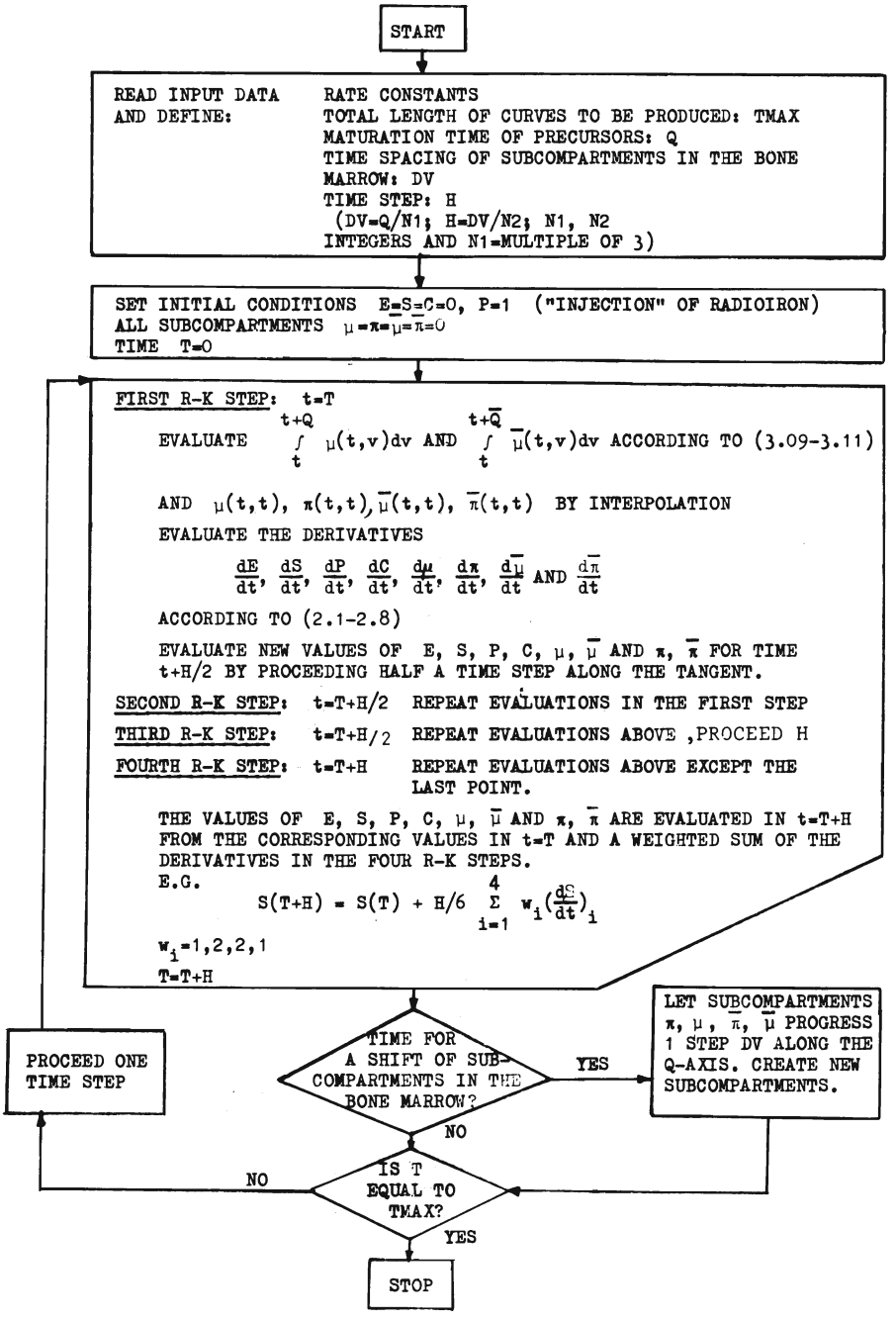


Fig. 9. The general principles of method B presented as a block-diagram.

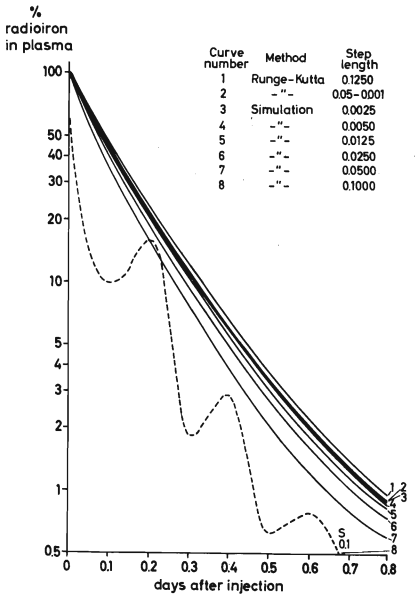


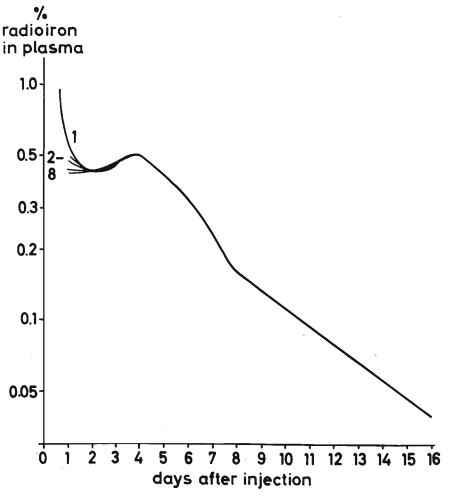


Fig. 10a. The disappearance curve as calculated with various step-lengths and parameters according to table 1. $t = 0 - 0.8$ days.
Fig. 10b. The disappearance curve as calculated with various step-lengths and parameters according to table 1. $t = 1 - 16$ days.
Curve numbers as in fig. 10a.

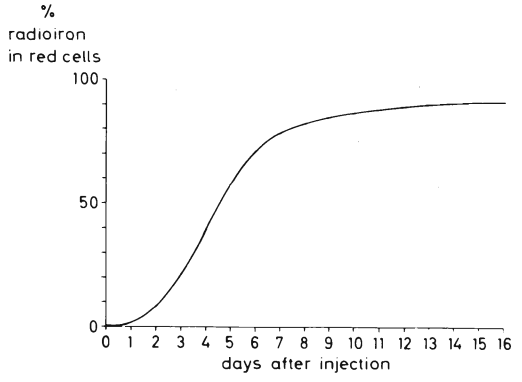


Fig. 11. The appearance curve.

Table 2
Accuracy of the two methods on the basis of model 1. The disappearance curve. "True" curve obtained from analytical expression.

| Method | Step length (days) | Maximum deviation (%) from "true" disappearance curve. |
|---|---|---|
| A | 0.005 | 5.5 |
| | 0.002 | 3.0 |
| | 0.001 | 1.5 |
| B | 0.01 | 4.5 |
| | 0.05 | 0.2 |

ber of similar curves (parameter estimation) it is suitable to choose two different step lengths and switch the step length after a certain time. In the present case, $t = 1$ day was found to be optimal for switching the steplength. The optimal "switch-point" may be different for different models and different parameter combinations, but can easily be found empirically.

The convergence properties of the two methods can suitably be investigated using model 1, for which "true" reference curves can be obtained from the analytical expressions in reference [1]. It was found that with decreasing $dt$ both methods yielded curves that in every part converged towards the "true" curves. For the disappearance curve, the maximum deviation from the true curve is shown in table 2. Table 3 shows the corresponding results for the appearance curve; for this curve, the accuracy is defined as the deviation at $t = 1$ day, since the maximum deviation always oc-

Table 3
Corresponding data to those in table 2 for the appearance curve

| Method | Step length | Deviation (%) from "true" appearance curve at $t$ = 1 day |
|---|---|---|
| A | 0.005 | 2.0 |
| | 0.002 | 1.5 |
| | 0.001 | 1.0 |
| B | 0.1 | 0.2 |

curred at $t < 1$ day, a region of the curve with no practical importance. From these tables it can also be seen that method B converges much more rapidly towards the "true" curve than method A, requiring considerably less computer time. With the conditions that $\bar{Q} = Q$ and $\bar{\omega} = \omega$, model 2 and model 3 yield identical curves. Because of the double number of subcompartments $\mu$ and $\pi$ in model 3, however, the computer time needed for the production of one set of curves is increased by a factor of almost 2. Therefore model 3 should only be applied in cases, where the experimentator has got a wellfounded hypothesis concerning the kinetics of maturation of "sick" precursors. In this case, the same conclusions as regards computer economy of the methods A and B will apply, as were obtained on the basis of model 2.

## 4. Hardware and software specifications

All the programs are coded in FORTRAN IV for the CD 3600 computer at the Uppsala University Data Center, Uppsala, Sweden. The computer is a 32K, 48 bits/word computer equipped with 2 magnetic drum storages (524K each) and 6 tape drives. Storage requirements and time for sample runs:

Model 3: Method A ~ 10K, c. 4 sec.
Method B ~ 5K, c. 90 sec.

The storage requirements are highly dependent on the number of subcompartments in the bone marrow compartment.

## 5. Mode of availability

The programs are available from Uppsala University Data Center Box 2103, 750 02 Uppsala, Sweden.

## References

[1] L.Garby, W.Schneider, O.Sundquist and J.-C.Vuille, Acta Physiol. Scand. 59, Suppl. 216 (1963).
[2] M.Pollycove and R,Mortimer, J. Clin. Invest. 40 (1961) 753.
[3] J.-C.Vuille, Acta Physiol. Scand. 65, Suppl. 253 (1965) 3.
[4] J.-C.Vuille, Acta Physiol. Scand. 65, Suppl. 253 (1965) 63.
[5] W.Jentsch, Digitale simulation kontinuerlicher Systeme (R. Oldenbourg Verslag, München, Wien, 1969).
[6] M.Berman, E.Shahn and M.F.Weiss, Biophys. J. 2 (1962) 275.
[7] Y.Chu, Digital simulation of continuous systems (McGraw–Hill, New York, 1969).
[8] L.G.Israels, J.Skandenberg, H.Guyda, W.Zingg and A. Zipursky, Brit. J. Haemat. 9 (1963) 50.
[9] I.M.London, R.West, D.Shemin and D.Rittenberg, J. Biol. Chem. 184 (1950) 351.
[10] T.Yamamoto, J.Skandenberg, A.Zipursky and L.G. Israels, J. Clin. Invest. 44 (1965) 31.

Program listing Method A:

```
      PROGRAM MODEL 3
      IRON-FLOW IN THE HUMAN BODY,METHOD A
C      READ INPUT DATA        TMAX=TOTAL LENGTH OF CURVES TO BE PRODUCED
C                             TSHIFT=TIME FOR CHANGE OF TIMESTEP
C                             DT1=TIME STEP BEFORE T=TSHIFT
C                             DT3=TIME STEP AFTER T=TSHIFT
C                             NF=NUMBER OF SUBCOMPARTMENTS IN BONE MARROW POOL
C                             DT2=TIME INTERVAL IN WHICH B.MARROW POOL IS DIVIDED
C                           **OBS**  DT2=P2/NF
C                           **OBS** DT1 AND DT3 LESS OR EQUAL TO DT2
C                                   DT2/DT1 AND DT2/DT3 MUST BE INTEGERS
C                             P2=Q IN PARAM.LIST=MATURATION TIME FOR PRECURSORS
C                             P1 DEFINES THE POSITION OF THE TOP OF TRIANGULAR
C                             DISTRIBUTION FUNCTIONS
C                           **OBS** INTHIS PROGRAM P1,P2 ARE THE SAME FOR SICK
C                             AND NORMAL PRECURSORS.WHEN OF INTEREST THIS MAY
C                             EASILY BE CHANGED
C                             S1,.......S7=RATE CONSTANTS
C                             S6=PART OF IRON FROM  PLASMA TO COMPARTM. SICK CELL
C                             IX,IY ARE PRINT INDICATORS. PRINTING OCCURS EVERY
C                             IX TH(BEFORE TSHIFT) RESP. IY TH(AFTER TSHIFT) STEP
      DIMENSION AFACH(1000),DD(1000),EE(1000),AFACH2(1000),DD2(1000),
     1EE2(1000)
   60 READ(60,1002) S1,S2,S3,S4,S5,S6,S7
      WRITE(61,1020)
 1020 FORMAT(1H1)
      WRITE(61,1004)S1,S2,S3,S4,S5,S6,S7
 1004 FORMAT(5X,*RATE CONSTANTS*/(3E20.10))
      IF(S7)61,61,62
 1002 FORMAT(8F10.0)
   62 READ(60,1001) IX,IY
      WRITE(61,1005) IX,IY
 1005 FORMAT(5X,*PRINT INDICATORS*,2I10)
      READ(60,1000)TMAX,DT1,DT2,TSHIFT,DT3
 1000 FORMAT(8F10.0)
      WRITE(61,1007)TMAX,DT1,DT2,TSHIFT,DT3
 1007 FORMAT(5X,*TIME PARAMETERS*/(3E20.10))
      READ(60,1008)NF,P1,P2
 1008 FORMAT(I10,2F10.0)
      WRITE(61,1009) NF,P1,P2
 1009 FORMAT(5X,*DATA FOR DISTR.FUNCTION*,I10,2F10.2)
      WRITE(61,1011)
 1011 FORMAT(////)
      WRITE(61,1006)
 1006 FORMAT(5X,*IRON-FLOW IN THE HUMAN BODY,DIRECT SIMULATION,MODEL 3*)
 1001 FORMAT(3I10)
      WRITE(61,1010)
 1010 FORMAT(6X,3H T ,6X,1HE,7X,5H  S  ,4X,6HPLASMA,4X,8HB.MARROW,2X,
     15HBLOOD )
      DEFINE THE DISTRIBUTION FUNCTIONS,HERE OF TRIANGULAR FORM
      DO 12 I=1,NF
      AI=I
      P=DT2*(AI-0.5)
      IF(P-P1)10,10,11
```

```
   10 AFACH(I)=2.*P*DT2/(P1*P2)*(1.-S6)
      AFACH2(I)=2.*P*DT2/(P1*P2)*S6
      GO TO 12
   11 AFACH(I)=2.*(P2-P)*DT2/(P2*(P2-P1)) *(1.-S6)
      AFACH2(I)=2.*(P2-P)*DT2/(P2*(P2-P1))*S6
   12 CONTINUE
      DEFINE INITIAL CONDITIONS OF ALL POOLS
                                A=POOL E IN FIGURE 3
                                B=POOL S
                                C=POOL P
                                D=POOL M, DD=SUBCOMPARTMENTS IN D
                                E=POOL PR, EE=SUBCOMPARTMENTS OF E
                                DE=D+E= THE BONE MARROW COMPARTMENT
                                INDEX 2 FOR SICK CELLS,E2,D2,EE2,DD2

C                               FG=POOL C
C     DEFINE TIME,TIMESTEP,TIME FOR SHIFT OF SUBCOMPARTMENTS IN B.MARROW POOL
C     INJECT RADIOIRON (TOTAL AMOUNT=1) INTO PLASMA POOL
      DO 20 I=1,NF
      DD(I)=0.
      DD2(I)=0.
      EE2(I)=0.
   20 EE(I)=0.
      DT=DT1
      T=0.
      TVER=DT2
      A=0.
      B=0.
      C=1.
      D=0.
      E=0.
      D2=0.
      E2=0.
      F=0.
      G=0.
      FG=0.
      DE=0.
      DE2=0.
      POOLS=1.
      NR=0
      AUS=1.-(S5+S7)*DT
      EIN=S7*DT
   30 IF(NR-NR/IX*IX)40,32,40
   32 WRITE(61,1003)T,A,B,C,BENM,FG
 1003 FORMAT(F10.2,6F10.6)
      IF(ABS(POOLS-1.)-1.E-6) 40,40,42
   42 WRITE(61,1012)POOLS
 1012 FORMAT(5X,*OBS SUM OF ALL COMPARTMENTS=*,E20.10)
C     INCREASE TIME BY DT
   40 T=T+DT
      REIN=C*S4*DT
C     CALCULATE AMOUNT FLOWING  FROM AND TO THE VARIOUS COMPARTMENTS
C     AND ADD -SUBTRACT FROM THE POOLS
C     DISTRIBUTE AMOUNT FLOWING TO PR AMONG SUBCOMPARTMENTS ACCORDING TO THE
C     RESPECTIVE UPTAKE RATES
      DO 41 I=1,NF
      EE2(I)=EE2(I)+DD2(I)*EIN
      DD2(I)=DD2(I)*AUS+AFACH2(I)*REIN
      EE(I)=EE(I)+DD(I)*EIN
```

```
   41 DD(I)=DD(I)*AUS+AFACH(I)*REIN
      E=E+D*EIN
      E2=E2+D2*EIN
      DALT=D
      DALT2=D2
      D=D*AUS+REIN*(1.-S6)
      D2=D2*AUS+REIN*S6
      A=A+B*S1*DT
      BALT=B
      B=B+(C*S2-B*(S1+S3))*DT
      C=C+(DALT*S5+DALT2*S5+BALT*S3-C*(S2+S4))*DT
   44 IF(TVER-T)46,46,52
C     LET SUBCOMPARTMENTS PROGRESS 1 STEP ALONG THE Q-AXIS. ADD CONTENT OF LAST
C     SUBCOMPARTMENTS EE,DD,EE2,DD2 TO CIRCULATING BLOOD AND PLASMA.CREATE NEW
C     SUBCOMPARTMENTS
   46 TVER=TVER+DT2
  470 EEALT=EE(1)
      DDALT=DD(1)
      EEALT2=EE2(1)
      DDALT2=DD2(1)
   47 DO 51 I=2,NF
      EE(I-1)=EE(I)
      EE2(I-1)=EE2(I)
      DD2(I-1)=DD2(I)

   51 DD(I-1)=DD(I)
      EE(NF)=0.
      DD(NF)=0.
      EE2(NF)=0.
      DD2(NF)=0.
  430 D=D-DDALT
      D2=D2-DDALT2
      E2=E2-EEALT2
      E=E-EEALT
      E=E+DDALT
      G=G+EEALT
      C=C+EEALT2+DDALT2
   52 DE=D+E
      DE2=D2+E2
      BENM=DE+DE2
      EG=E+G
      POOLS=A+B+C+DE+EG+DE2
      NR=NR+1
C     TIMESTEP DT IS CHANGED WHEN T EQUAL TSHIFT
      IF(ABS(T-TSHIFT)-1.E-8) 45,45,59
   45 DT=DT3
      AUS=1.-(S5+S7)*DT
      EIN=S7*DT
      IX=IY
      NR=0
   59 IF(T-TMAX)30,30,60
   61 CALL EXIT
      END
```

Method A.

```
 RATE CONSTANTS
5,0000000000-002     1,5000000000+000     1,5000000000-001
7,5000000000+000     2,0000000000+000     1,0000000000-001
9,0000000000+000
 PRINT INDICATORS          4          20
 TIME PARAMETERS
2,0000000000-001     2,5000000000-002     1,0000000000-001
1,0000000000+000     5,0000000000-002
 DATA FOR DISTR,FUNCTION          75        3,75        7,50
```

IRON-FLOW IN THE HUMAN BODY,DIRECT SIMULATION,MODEL 3

| T | E | S | PLASMA | B,MARROW | BLOOD |
|---|---|---|---|---|---|
| 0,00 | 0,000000 | 0,000000 | 1,000000 | 0,000000 | 0,000000 |
| 0,10 | 0,000241 | 0,106748 | 0,393824 | 0,499028 | 0,000160 |
| 0,20 | 0,000868 | 0,149269 | 0,183945 | 0,665252 | 0,000665 |
| 0,30 | 0,001655 | 0,167821 | 0,093547 | 0,735384 | 0,001593 |
| 0,40 | 0,002512 | 0,175607 | 0,049869 | 0,769026 | 0,002986 |
| 0,50 | 0,003396 | 0,178122 | 0,027754 | 0,785861 | 0,004868 |
| 0,60 | 0,004287 | 0,177976 | 0,016105 | 0,796764 | 0,004868 |
| 0,70 | 0,005175 | 0,176480 | 0,010189 | 0,800903 | 0,007254 |
| 0,80 | 0,006053 | 0,174316 | 0,007109 | 0,802369 | 0,010153 |
| 0,90 | 0,006920 | 0,171834 | 0,005504 | 0,802171 | 0,013571 |
| 1,00 | 0,007774 | 0,169215 | 0,004668 | 0,800833 | 0,017510 |
| 2,00 | 0,015621 | 0,144147 | 0,003858 | 0,750359 | 0,086015 |
| 3,00 | 0,022327 | 0,123901 | 0,004043 | 0,641106 | 0,208623 |
| 4,00 | 0,028126 | 0,107943 | 0,004299 | 0,473140 | 0,386493 |
| 5,00 | 0,033204 | 0,094772 | 0,004751 | 0,287806 | 0,579466 |
| 6,00 | 0,037651 | 0,082619 | 0,003646 | 0,169486 | 0,706598 |
| 7,00 | 0,041513 | 0,071408 | 0,002530 | 0,099102 | 0,785447 |
| 8,00 | 0,044832 | 0,060993 | 0,001660 | 0,074176 | 0,818339 |
| 9,00 | 0,047659 | 0,051877 | 0,001420 | 0,059000 | 0,840044 |
| 10,00 | 0,050064 | 0,044128 | 0,001201 | 0,045989 | 0,858617 |
| 11,00 | 0,052109 | 0,037521 | 0,001001 | 0,035865 | 0,873504 |
| 12,00 | 0,053848 | 0,031879 | 0,000829 | 0,028515 | 0,884930 |
| 13,00 | 0,055324 | 0,027065 | 0,000690 | 0,023218 | 0,893703 |
| 14,00 | 0,056577 | 0,022966 | 0,000579 | 0,019240 | 0,900638 |
| 15,00 | 0,057641 | 0,019483 | 0,000488 | 0,016076 | 0,906312 |
| 16,00 | 0,058543 | 0,016527 | 0,000413 | 0,013461 | 0,911056 |
| 17,00 | 0,059308 | 0,014018 | 0,000350 | 0,011295 | 0,915029 |
| 18,00 | 0,059957 | 0,011887 | 0,000274 | 0,009828 | 0,918054 |
| 19,00 | 0,060507 | 0,010082 | 0,000232 | 0,008269 | 0,920910 |
| 20,00 | 0,060973 | 0,008551 | 0,000197 | 0,006956 | 0,923322 |

```
Method B

 RATE CONSTANTS
5,0000000000-002     1,5000000000+000     1,5000000000-001
7,5000000000+000     2,0000000000+000     1,0000000000-001
9,0000000000+000
 TIME VARIABLES
   300          1          60          4          8
 Q,QS,DEL,     7,5000000000+000     7,5000000000+000     1.0000000000+000
 TMAX,TSHIFT     2,0000000000+001     1,0000000000+000


 IRON-FLOW IN THE HUMAN BODY,MODEL 3,RUNGE-KUTTA METHOD
 DV,H     2,5000000000-002     2,5000000000-002
   T          E          S          BLOCD     B,MARROW    PLASMA
 0,000000                                     0,000000
 0,100000  0,000285   0,099665   0,000080                 0,436149
 0,100000                                     0,463820
 0,200000  0,000907   0,143502   0,000450                 0,212655
 0,200000                                     0,642485
 0,300000  0,001681   0,163778   0,001211                 0,111296
 0,300000                                     0,722030
 0,400000  0,002526   0,172902   0,002416                 0,060985
 0,400000                                     0,761168
 0,500000  0,003401   0,176374   0,004096                 0,034723
 0,500000                                     0,781402
 0,600000  0,004285   0,176885   0,006270                 0,020669
 0,600000                                     0,791888
 0,700000  0,005167   0,175828   0,008949                 0,013061
 0,700000                                     0,796991
 0,800000  0,006042   0,173947   0,012141                 0,008925
 0,800000                                     0,798942
 0,900000  0,006906   0,171643   0,015852                 0,006674
 0,900000                                     0,798921
 1,000000  0,007758   0,169135   0,020084                 0,005453
 1,000000                                     0,797594
 2,000000  0,015579   0,144336   0,091568                 0,004221
 2,000000                                     0,744294
 3,000000  0,022272   0,124165   0,217270                 0,004605
 3,000000                                     0,631673
 4,000000  0,028066   0,108246   0,397485                 0,005005
 4,000000                                     0,461176
 5,000000  0,033140   0,094936   0,572745                 0,004223
 5,000000                                     0,294955
 6,000000  0,037579   0,082820   0,702133                 0,003300
 6,000000                                     0,174175
 7,000000  0,041437   0,071639   0,783328                 0,002365
 7,000000                                     0,101200
 8,000000  0,044756   0,061246   0,817858                 0,001592
 8,000000                                     0,074537
 9,000000  0,047584   0,052130   0,839723                 0,001352
 9,000000                                     0,059200
10,000000  0,049992   0,044371   0,858372                 0,001145
10,000000                                     0,046107
11,000000  0,052040   0,037750   0,873294                 0,000957
```

| | | | | | |
|---|---|---|---|---|---|
| 11,000000 | | | | 0,035945 | |
| 12,000000 | 0,053783 | 0,032092 | 0,884718 | | 0,000796 |
| 12,000000 | | | | 0,028597 | |
| 13,000000 | 0,055263 | 0,027263 | 0,893485 | | 0,000665 |
| 13,000000 | | | | 0,023310 | |
| 14,000000 | 0,056521 | 0,023148 | 0,900411 | | 0,000559 |
| 14,000000 | | | | 0,019347 | |
| 15,000000 | 0,057588 | 0,019649 | 0,906076 | | 0,000473 |
| 15,000000 | | | | 0,016199 | |
| 16,000000 | 0,058494 | 0,016678 | 0,910812 | | 0,000400 |
| 16,000000 | | | | 0,013601 | |
| 17,000000 | 0,059264 | 0,014155 | 0,914779 | | 0,000339 |
| 17,000000 | | | | 0,011449 | |
| 18,000000 | 0,059916 | 0,012013 | 0,918106 | | 0,000287 |
| 18,000000 | | | | 0,009663 | |
| 19,000000 | 0,060470 | 0,010194 | 0,920905 | | 0,000243 |
| 19,000000 | | | | 0,008172 | |
| 20,000000 | 0,060940 | 0,008650 | 0,923267 | | 0,000206 |
| 20,000000 | | | | 0,006920 | |